Interference Path Loss Prediction in A319/320 Airplanes Using Modulated Fuzzy Logic and Neural Networks

Madiha J. Jafri
Dept. of Electrical Eng.
Old Dominion University
Norfolk, VA 23529, USA
madiha.jafri@gmail.com

Jay J. Ely
High Intensity Radiated Fields Lab
NASA Langley Research Center
Hampton, VA, 23681, USA
j.j.ely@larc.nasa.gov

Linda L. Vahala
Dept. of Electrical Eng.
Old Dominion University
Norfolk, VA 23529, USA
lvahala@odu.edu

***Abstract* – In this paper, neural network (NN) modeling is combined with fuzzy logic to estimate Interference Path Loss measurements on Airbus 319 and 320 airplanes. Interference patterns inside the aircraft are classified and predicted based on the locations of the doors, windows, aircraft structures and the communication/navigation system-of-concern. Modeled results are compared with measured data. Combining fuzzy logic and NN modeling is shown to improve estimates of measured data over estimates obtained with NN alone. A plan is proposed to enhance the modeling for better prediction of electromagnetic coupling problems inside aircraft.**

I. Introduction

There has been an increased concern about electromagnetic interference (EMI) caused by the use of Portable Electronic Devices (PEDs) onboard commercial airplanes. PEDs may act as transmitters, both intentional and unintentional, and their signals may be detected by various receivers on the aircraft. Researchers at NASA Langley Research Center, Eagles Wings Incorporated, and United Airlines have collected measurement data in an effort to understand the EMI patterns on aircraft. Previous publications include graphical and statistical models of Interference Path Loss (IPL) on several United B737 airplanes [1]. IPL is the measurement of the radiated field coupling between passenger cabin locations and aircraft communication and navigation receivers, via their antennas. The measurement is required for assessing the threat of PEDs to aircraft radios, and is very dependant upon airplane size, the interfering transmitter's position within the aircraft, and the location of the particular antenna for the aircraft system of concern. To date, no modelling technique has been successfully used to predict indoor-outdoor coupling phenomenon for aircraft. In this paper, a modulated neural network and fuzzy logic model is introduced that utilizes measured IPL data and incorporates expert knowledge to effectively model coupling patterns inside A319 and A320 airplanes.

II. Testing Methodology

Before attempting to understand the analysis of IPL data, it is necessary to review how the data was measured. IPL, as addressed herein, is particularly focused upon in-band, on-channel type EMI to aircraft radios, via their antennas. This does not include EMI to aircraft radios outside their radio frequency (RF) passband, and does not include radiated field (or conducted) coupling to wiring and equipment apertures.

A. IPL Data

IPL data were taken by radiating a low powered test signal, frequency-synchronized to the spectrum analyzer sweep and fed to the test transmitting antenna via a double-shielded RF cable. The spectrum analyzer, laptop computer controller, signal generators, RF amplifiers and preamplifiers were located inside the aircraft passenger cabin. The spectrum analyzer input cable was connected to the aircraft radio receiver rack cable in the avionics equipment bay.

To perform an IPL measurement, the RF power loss was measured between the calibrated signal source and a spectrum analyzer, via the entire length of test cables plus the aircraft cable, plus the free space loss between the reference antenna and the aircraft antenna. For calibration, test cable losses were measured separately by connecting the two ends of the test cables to the input and output of the spectrum analyzer, and subtracting this loss, in dB, from the raw measurement. Individual IPL measurements were obtained by moving the test antenna from one window to the next, throughout the airplane. Additional data and measurement details may be found in [2-7].

B. Test Systems and Locations

IPL measurements were taken at all window locations of A319 and A320 airplanes. From an electromagnetic coupling point-of-view, A319 and A320 airplanes are structurally different, with different numbers of windows and exits, as well as with aircraft antennas installed at different locations. Figure 1 shows a side view of the A319 and A320. As described previously, IPL measurements were taken with respect to each of the systems pointed to in Figure 1. Measurements were performed at each window location of the aircraft, on both port and starboard side, resulting in 32 measurements for the A319 and 40 measurements for the A320. Table 1 includes a list of the systems tested along with their operating frequencies.

TABLE 1: Frequency Ranges of Systems tested

Aircraft Systems	Frequency Range
LOC: Instrument Landing System Localizer	108-118 MHz
GS: Glide Slope	325-340 MHz
DME: Distance Measuring Equipment	960-1215 MHz
ATC: Air Traffic Control transponder	1090 MHz
VHF: Very High Frequency communication	118-138 MHz

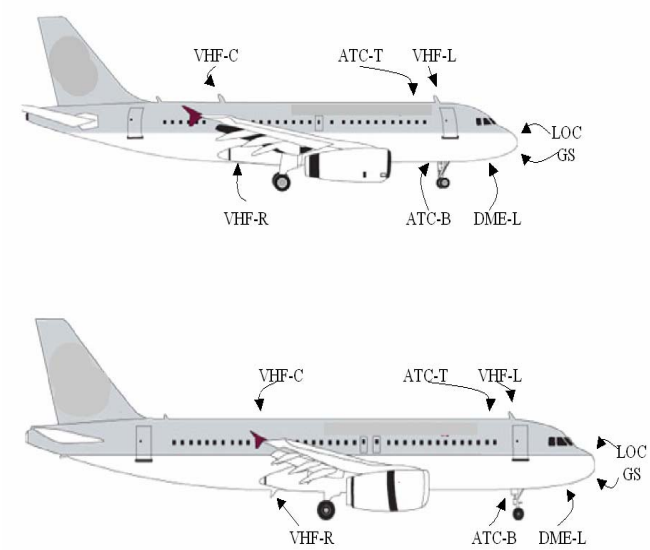

Fig. 1 Aircraft systems tested on A-319 (top) and A-320 (bottom)

IPL data were taken on both port and starboard sides of the aircraft. Due to the symmetry of the aircraft, the two measurement sets from port and starboard were considered two trials for each system, instead of two independent measurements. Eight systems were tested on the A319 (with two trials each for port and starboard, resulting in 16 datasets for the A319). Seven systems (with two trials) were tested on the A320, resulting in 14 datasets. Therefore, a total of 30 datasets were available for training and testing of neural networks as explained in the next sections. For each of the 30 datasets, data was taken in both vertical and horizontal polarizations.

III. Modulated Neuro-Fuzzy Modeling (NFM)

Modeling techniques, such as ray tracing and fuzzy logic, have been proposed to study the interference patterns inside commercial aircraft due to PEDs [8]; however, we suggest that a combination of neural networks and fuzzy logic provide useful results with as little computational effort as possible [9]. Neural networks not only have the capability to learn various interference patterns according to the locations of doors, windows and aircraft antenna location, but they also learn interference patterns from one aircraft to the other. This dynamic capability can significantly improve modeling accuracy for other aircraft, which may eventually eliminate the need to take time consuming and tedious IPL measurements of other aircraft. Fuzzy logic, on the other hand, incorporates expert knowledge into the modelling which may not be apparent to the neural-network module of the modelling.

A. Introduction to Neural Networks

Feed-forward neural networks have been widely used for various tasks, such as pattern recognition, function approximation, dynamical modeling, data mining, time-series forecasting and more. Many solutions in different fields have been obtained that were otherwise impossible through other modeling techniques, such as Markov models and complex computational models. NNs can be used in a variety of powerful ways: to learn and reproduce rules or operations from given examples; to analyze and generalize from sample facts and make predictions from these; or to memorize characteristics and features of given data and to match or make associations from new data to the old data.

The backpropagation algorithm is the most important algorithm for the supervised training of multi-layer feed-forward NNs. It derives its name from the fact that error signals are propagated backward through the network on a layer-by-layer basis. The backpropagation algorithm is based on the selection of a suitable error function or cost function, whose values are determined by the actual and desired outputs of the network and which is also dependant on the network parameters such as the weights and the thresholds.

The layer which intakes the input values is known as the input layer; similarly, the last layer is known as the output layer. The layers in between the input and output layers are known as hidden layers and consist of several nodes. Figure 2 is a good illustration of a feed-forward neural network structure in which three layers are shown. The dashed arrows going upward show the application of the backpropagation algorithm used to update the two weight matrices labeled at the two interconnections of the three layers.

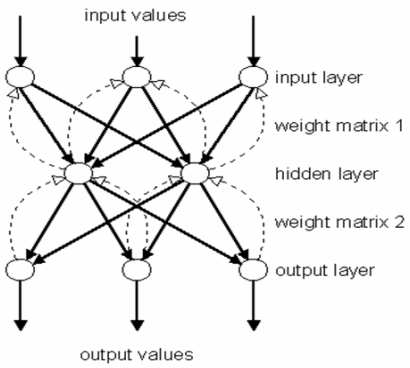

Fig. 2: Feed Forward Neural Network

The main goal of backpropagation is to train weights such that they minimize the squared error described as follows:

$$E = \frac{1}{2}\sum_{n=1}^{N}\sum_{k=1}^{K}[y_k^n - f_k(x^n)]^2$$

where n is the number of training samples, k is the number of output units; the values being subtracted are y_k, the target output with $f_k(x)$, which is the output produced by the NN undergoing training or testing. In back propagation, the weights of the network are updated starting with the hidden to output weights, followed by the input to hidden weights, with respect to the sum of square error mentioned above and through a series of weight update rules, called the delta rules.

B. Introduction to Fuzzy Logic

Fuzzy Logic provides a simple way to arrive at a definite conclusion based upon vague, ambiguous, imprecise, noisy or missing input information. The logic extends Boolean logic to handle the expression of vague concepts. To express imprecision in a quantitative fashion, it introduces a set of membership functions that map elements to real values between zero and one (inclusive); the values indicate the "degree" to which an element belongs to a set. A membership value of zero indicates that the element is entirely outside the set, whereas a one indicates that the element lies entirely inside a given set. Any value between the two extremes indicates a degree of partial membership to the set.

The four-step fuzzy reasoning procedures employed by applications includes: Fuzzification, which establishes the fact base of the fuzzy system. First, it identifies the input and output of the system and then identifies the appropriate if-then rules and uses raw data to derive a membership function. At this point, one is ready to apply the fuzzy logic to the system. As inputs are received by the system, inference, the second step, evaluates all if-then rules and determines their truth values. If a given input does not precisely correspond to an if-then rule, then partial matching of the input data is used to interpolate an answer. Then composition, the third step, combines all fuzzy conclusions obtained by inference into a single conclusion. Different fuzzy rules might have different conclusions, so it is necessary to consider all rules. The final step of defuzzification converts the fuzzy value obtained from composition into a "crisp" value; this process is often complex since the resulting fuzzy set might not translate directly into a crisp value. Defuzzification is necessary, since controllers of physical systems require discrete signals.

C. Modulated Fuzzy Logic with Neural Networks

Fuzzy logic and neural networks were combined in modulated components to lead to the most optimal IPL predictions. Below are details of each of the 5 modules:

Module 1: As mentioned earlier, IPL patterns are heavily dependent on the location of the doors, windows and aircraft antennas. Therefore, before initiating the modeling process, the distance and angle calculations were performed to locate the doors, windows and aircraft antenna systems relative to each other. Therefore, in this module, aircraft characteristics (summarized in table 2) were used as inputs to calculate distances and angles of each aircraft window to doors and antenna locations. Distance with respect to aircraft antenna (i.e. from measurement location to aircraft antenna) was calculated using parametric formula of an ellipse (drawn in Fig. 3).

$$D = \frac{1}{4} * \pi \left[3(a+b) - \sqrt{(3a+b)(a+3b)} \right]$$

$$\alpha = \cos^{-1}\left(\frac{b}{a}\right), \beta = \tan^{-1}\left(\frac{b}{x}\right)$$

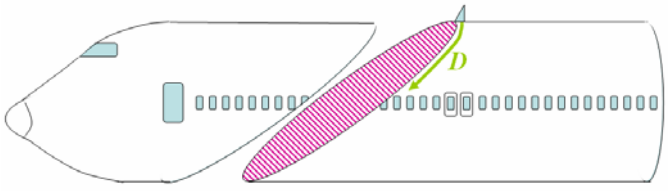

Fig. 3: Visualization of cutting cylindrical fuselage

Where D represents calculated distance from aircraft antenna to test window; a and b are major and minor axis (respectively) of the ellipse; x is the distance from test window to window closest to aircraft antenna; α is the angle calculated between antenna (mounted on fuselage) and test window, while β is the angle calculated between antenna (mounted on nose) to fuselage.

Also, as the A319 and A320 vary in length and thus in number of windows, every 4th window in A319 was duplicated to ensure equal lengths of 40 windows in both A319 and A320.

TABLE 2
INPUT CHARACTERISTICS FOR F-NN MODEL

Features	A319	A320
Aircraft Length (cm)	3383	3750
Port vs. Starboard	1 or 0	1 or 0
Number of Windows	32	40
Exit 1 location	767	780
Exit 2 location	2810	3050
Emergency Exit 1 loc.	1604	1002
Emergency Exit 2 loc.	1604	1709
Aircraft system loc. (x)	200 → 3383	200 →3750
Aircraft system loc. (y)	-206.8 → +206.8	-206.8 →+206.8
Aircraft system loc. (z)	-15 →+15	-15 →+15
Op. freq. (start, MHz)	108→1565	108→1565
Op. freq. (stop, MHz)	108→1585	108→1585
System's dominant pol.	H (0) or V (1)	H (0) or V (1)

Module 2: In the second module, all distance values measured in the previous module were read and fuzzy rules were applied to determine IPL pattern. Three specific fuzzy rules were created. The first rule estimated IPL values based on the measurement location with respect to location of the exits and emergency exits. As the distance from exits increased, the value of coupling was expected to decrease. Figure 4 (top, bottom) shows the two variations on Rule 1 (for main exit and emergency exit, respectively). It can be observed that we expect coupling to decrease slightly faster

through emergency exits than main doors as we predict that main doors are leakier than emergency exits.

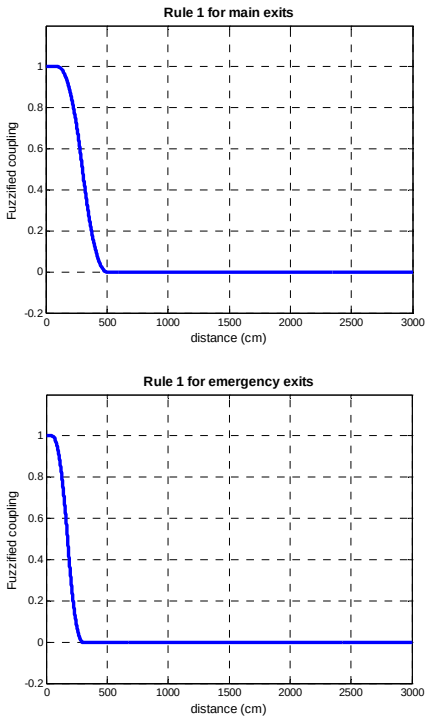

Fig. 4: Coupling rule based on location of doors (*top*: main exit, *bottom*: emergency exits) with respect to seat locations

The second rule (Fig. 5) predicted IPL values by comparing distance from measurement location to the location of the aircraft antenna either on top or bottom of the fuselage, using calculated *D* values from previous equation.

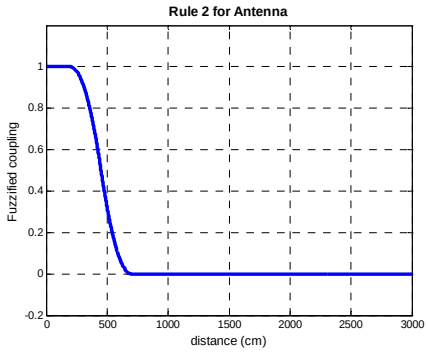

Fig. 5: Coupling rule based on location of Aircraft Antenna with respect to seat locations

Finally, the last rule utilized the aircraft system's dominant polarization (dominant or vertical based on the last row in Table 2) to determine whether the IPL value will increase or decrease based on the angle between the measured seat location and the aircraft antenna (Fig. 6). Distance values from angles α and β were derived and used in the rules (x-axis) based on whether the system was mounted on the nose, or the fuselage (non-nose) of the aircraft. Three variations of Rule 3 were created: First, for systems mounted on the fuselage (non-nose) with dominant vertical polarization (i.e ATC, DME and VHF). Second, for systems mounted on the fuselage (non-nose) with dominant horizontal polarization. (ie. LOC on tail of aircraft. This rule was not used in this simulation.) Third, for systems mounted on the nose with dominant horizontal polarization (i.e. GS and LOC). No rule was required for systems mounted in the nose with dominant vertical polarization because this combination does not exist in our datasets. The results from all rules were added together to pass on a single array of IPL values to the next module.

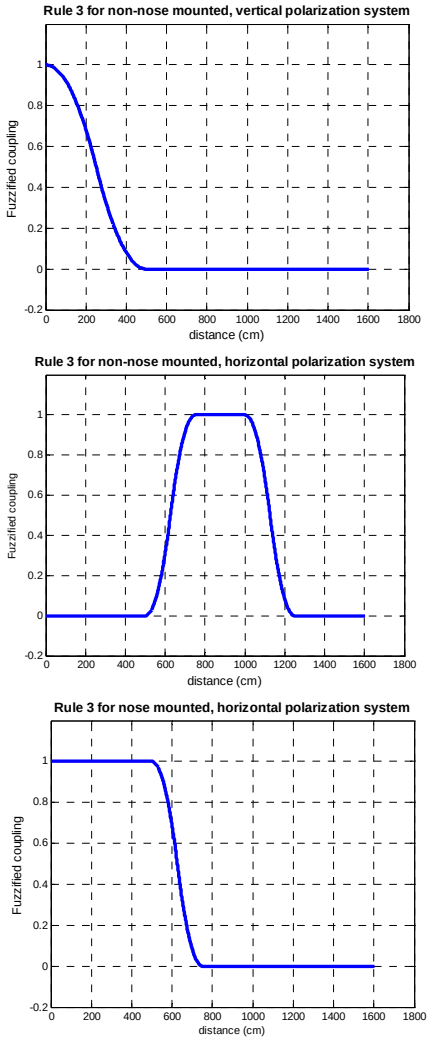

Fig. 6: Coupling rules based on dominant polarization and distance from angle of the antenna with respect to seat locations

Module 3: The outputs from the fuzzy logic module needed to be defuzzified based on actual measured IPL data. However, instead of creating a linear defuzzification mapping function, we created a small neural network structure that predicted the maximum and minimum IPL value for a particular system based on the aircraft length, as well as the start and stop frequency for the aircraft system of concern. Therefore, this module read in the aircraft characteristics and predicted the minimum and maximum IPL values.

Module 4: In this module, the outputs from the neural networks (from Module 3) were used to create a linear transformation function for the defuzzification of the IPL values generated in Module 2.

Module 5: This module consisted of the main neural network simulation, in which the 20 defuzzified IPL values (every other IPL value from the 40 outputs) from Module 4 were sent in as inputs of the neural network, while the output consisted of the IPL values for the 20 windows. Therefore, we created a 20 input, 30 hidden and 20 output neural network structure for our simulation. By passing the defuzzified IPL pattern through neural networks, we hoped to incorporate the non-linear relationships among the various windows into our system. Finally, the 20 IPL values from the neural network output were interpolated to fit a 40 window aircraft.

IV. Neuro-Fuzzy Modeling Results

In order to test the above design, IPL data was used to train the NFM, and then testing was performed to estimate the accuracy of the trained NFM. Training data inputs and outputs were used to set the weights of the neural networks properly, with the goal of minimizing the error rate. Once the weights were set (using the training set's outputs and back propagation algorithm), testing data input was passed through the NFM structure, and the computed outputs were compared with actual testing data's outputs to determine the accuracy of the NFM prediction. Table 3 shows the systems tested for each aircraft type.

TABLE 3
AVAILABLE DATA FROM EACH AIRCRAFT TYPE

A319	A320
ATC-B	ATC-B
ATC-T	ATC-T
DME-L	DME-L
GS-L	GS-L
LOC-L	LOC-L
VHF-C	VHF-C
VHF-L	VHF-L
VHF-R	

Fifteen NFM simulations were performed as per the availability of data in Table 3. In each simulation, one system was reserved as test system, while all the other fourteen systems were used to train the neural networks. For example, for the first simulation, A319's ATC-B was reserved to test the NFM, while all other systems (A319's ATC-T, DME-L, GS-L, LOC-L, VHF-C, VHF-L, VHF-R, A320's ATC-B, ATC-T, DME-L, GS-L, LOC-L, VHF-C and VHF-L) were used to train the neural networks in the model.

Figure 7 shows a sample NFM output in which A319's VHF-L is used as testing data, while the other systems are used in training the neural networks in NFM. The light (green) lines represent the training data (from the other fourteen systems in the training set), while the solid (red) represents the test data (unknown to the NFM). The dashed line (red) represents the NFM predictions, based on the 13 inputs of the test dataset.

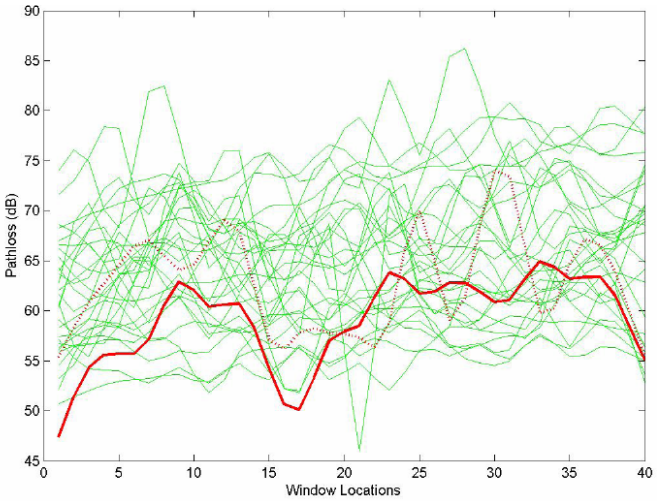

Fig. 7: Sample Simulation for A319's VHF-L (vertical polarization). Green=training data (all systems), Solid Red=VHF-L measured data, Dashed Red=NFM prediction

Table 4 shows the means and standard deviations for actual IPL data versus NFM simulated IPL data for all fifteen simulations. In previous work [10], we performed IPL prediction using only neural networks, instead of modulated neural networks with fuzzy logic. For comparison purposes, the results from the previous NN simulations are also included (labeled 'NN'). For analysis purposes, we equate "improved performance" of one model over the other based on the estimates of the modeled mean that more closely matches the actual mean. In the table, values accompanied by an asterisk (*) represent the systems in which simple NN performed better in prediction than the new NFM. In previous NN-only simulations, ATC and DME-L predicted means and standard deviations compared very closely to measured data for both A319 and A320 airplanes. Unfortunately, ATC and DME-L did not yield the best predictions when using the new NFM. However, as seen in the table, the new NFM model performed better than NN-only modeling in most of the other simulations. NFM prediction errors will continue to decline as more training data is incorporated. Aside from the measurements marked with an '*', all other IPL predicted means deviated within 7dB from actual IPL values. Past comparisons of measurement data from B737 and B747 airplanes showed variations of 3 to 6 dB between similar airplanes, so 3 to 7 dB variations between NFM predictions and measured IPL data should be considered acceptable. [6, 7]

Previous work showed that the NN-only model performed very well in predicting DME-L IPL patterns for both A319 and A320 aircraft, even though the IPL means are 9dB apart between the two airplane models. This result showed that the NN was dynamically learning from other systems, instead of simply copying A320 DME-L results for A319 prediction and vice versa. The same dynamic learning applied to ATC-B for both aircraft. However, in the current NFM model, the predicted DME-L, ATC-T, and ATC-B mean IPL values are very close in both aircraft types (A319 and

A320). If more aircraft information is incorporated into the neural networks, improved differentiation among various tested aircraft may improve this result. Future efforts will likely include a special fuzzy rule for DME/ATC systems (both L-Band systems with operating frequencies greater than 800 MHz) to enhance the NFM model.

VHF-R was only tested on the A319 (and not on the A320); therefore, when testing the A319's VHF-R, the NFM did not have reference to another aircraft's VHF-R patterns. Learning from all non-VHF-R systems, the NFM was able to predict the A319's VHF-R pattern very accurately, with only a 0.4 dB mean difference. In the previous NN-only model, this difference was 5 dB.

TABLE 4:
IPL COMPARISON OF ACTUAL, NN AND NFM

	System	Actual Mean	NN Mean	NFM Mean	Actual Std.	NN Std.	NFM Std.
A320	ATC-B	70.6	67.2	67.2	4.5	6.2	5.3
	ATC-T	72.0	62.4	66.7	4.1	5.9	5.6
	DME-L	70.6	73.6	69.1	3.6	3.4	5.4
	GS-L	66.0	70.1	68.8	3.4	2.3	5.6
	LOC-L	69.6	61.5	64.4	4.6	7.9	6.5
	VHF-C	67.2	66.7	68.5	5.5	6.7	5.4
	VHF-L	65.1	71.1	68.8	3.7	6.2	5.1
A319	ATC-B	58.1	59.5	65.7*	2.5	1.3	6.2
	ATC-T	56.3	59.9	63.5*	1.7	1.5	6.5
	DME-L	61.6	63.6	66.7*	2.9	7.2	5.4
	GS-L	60.0	70.7	66.9	2.0	1.9	5.3
	LOC-L	67.8	55.3	63.2	3.1	2.6	5.3
	VHF-C	60.4	68.9	69.9*	3.8	4.9	3.9
	VHF-L	59.1	74.4	64.9	3.3	3.6	4.9
	VHF-R	65.9	60.3	65.5	4.9	2.0	6.5

V. CONCLUSION

Modeling of IPL inside commercial aircraft has been a concern for many years. Although several modeling techniques have been proposed, the techniques have been too complex or inflexible for practical application to various structurally different aircraft. Neural network modeling, based on artificial intelligence, is an excellent selection for this application, due to its ability to learn and predict various IPL patterns from one aircraft to another for various system antennas installed in different aircraft locations. Fuzzy Logic is also a good selection for this application because IPL measurement data have been the subject of extensive graphical analysis in previous years, thus providing an increased expert knowledge in the IPL predictions that can to be incorporated into the model.

The analysis presented in this paper shows that measurement data from two structurally different aircraft can be integrated together for effective learning. With careful simulations, the neural networks in the NFM were trained to predict IPL patterns inside commercial aircraft, depending on the locations of exits, locations of antennas, the length and structure of aircraft as well as the location, operating frequency and polarization of the aircraft system of concern. Incorporation of other aircraft measurement data, (ie. B757 and B737), should further enhance the modeling. Most importantly, the measurement and NFM simulation results are statistically comparable. Statistical comparisons are necessary for developing risk analyses for EMI caused by PEDs being used on board airplanes. It is expected that more data collection and incorporation of additional aircraft types will enhance the training of neural networks for better classification. This work will assist in modeling EMI patterns, as opposed to performing tedious and expensive measurements, based on the location of the transmitter, the size of the aircraft, and the locations of the aircraft's antennas and exits.

ACKNOWLEDGMENT

The data evaluated in this paper were obtained from a joint partnership between United Airlines, Eagles Wings Inc. and NASA's Aviation Safety Program. The authors specifically thank Mr. Gerald L. Fuller for his previous analysis of the data upon which this work builds.

REFERENCES

[1]. Jafri, Madiha, J. Ely, L. Vahala. "Graphical and Statistical Analysis of Airplane Passenger Cabin RF Coupling Paths to Avionics." 22nd DASC, Indianapolis, IN, October 12 – 16, 2003. http://techreports.larc.nasa.gov/ltrs/PDF/2003/mtg/NASA-2003-22dasc-mj.pdf

[2]. Fuller, Gerald. "B737-200 Path Loss Tests: Victorville, California." Mariposa, CA, March 2002, Task 1 report, NASA Contract L-16099

[3]. Horton, Kent; Huffman, Mitch; Eppic, Brian; White, Harrison, "757 Path Loss Measurements", NASA/CR-2005-213762, 20050601; June 2005. http://hdl.handle.net/2060/20050186545

[4]. RTCA/DO-233, "Portable Electronic Devices Carried on Board Aircraft", August 20, 1996.

[5]. Jafri, Madiha, J. Ely, L. Vahala. "Classification and Prediction of Interference Pathloss Measurements inside B757 Using Feed Forward Neural Networks." 12th Biennial IEEE Conf. on Electromagnetic Field Computation, Miami, FL, April 30 – May 3, 2006.

[6]. Fuller, Gerald, "B747-400 Path Loss Tests, Victorville, California, April 2002", NASA PO L-16099 Task 2, May 2002.

[7]. Fuller, Gerald, "B737-200 Path Loss Tests, Victorville, California, May 2002", NASA PO L-16099 Task 3, June 2002.

[8]. Jafri, Madiha, J. Ely, L. Vahala. "Fuzzification of Electromagnetic Interference Patterns Onboard Commercial Airliners due to Wireless Technology." IEEE A&P Conf., Monterey, CA, June 20—26 2004.

[9]. Zadeh, L and R. Yager. "Fuzzy Sets, Neural Networks, and Soft Computing." VNR Publishing, 1994.

[10]. Jafri, Madiha, J. Ely, L. Vahala. "Classification and Prediction of RF Coupling inside A-320 and A-319 Airplanes using Feed Forward Neural Networks." 25th DASC, Portland, OR, October 15—19 2006.